Published in final edited form as:
J Biol Chem. 2008 February 29; 283(9): 5542–5553. doi:10.1074/jbc.M705653200.

General Transcription Factor IIA-γ Increases Osteoblast-specific *Osteocalcin* Gene Expression via Activating Transcription Factor 4 and Runt-related Transcription Factor 2[*,S]

Shibing Yu[‡], **Yu Jiang**[§], **Deborah L. Galson**[‡], **Min Luo**[‡], **Yumei Lai**[‡], **Yi Lu**[‡], **Hong-Jiao Ouyang**[‡], **Jian Zhang**[‡], and **Guozhi Xiao**[‡,1]

[‡]Department of Medicine University of Pittsburgh, Pittsburgh, Pennsylvania 15240

[§]Department of Pharmacology, University of Pittsburgh, Pittsburgh, Pennsylvania 15240

Abstract

ATF4 (activating transcription factor 4) is an osteoblast-enriched transcription factor that regulates terminal osteoblast differentiation and bone formation. ATF4 knock-out mice have reduced bone mass (severe osteoporosis) throughout life. Runx2 (runt-related transcription factor 2) is a runt domain-containing transcription factor that is essential for bone formation during embryogenesis and postnatal life. In this study, we identified general transcription factor IIAγ (TFIIAγ) as a Runx2-interacting factor in a yeast two-hybrid screen. Immunoprecipitation assays confirmed that TFIIAγ interacts with Runx2 in osteoblasts and when coexpressed in COS-7 cells or using purified glutathione *S*-transferase fusion proteins. Chromatin immunoprecipitation assay of MC3T3-E1 (clone MC-4) preosteoblast cells showed that in intact cells TFIIAγ is recruited to the region of the *osteocalcin* promoter previously shown to bind Runx2 and ATF4. A small region of Runx2 (amino acids 258–286) was found to be required for TFIIAγ binding. Although TFIIAγ interacts with Runx2, it does not activate Runx2. Instead, TFIIAγ binds to and activates ATF4. Furthermore, TFIIAγ together with ATF4 and Runx2 stimulates *osteocalcin* promoter activity and endogenous mRNA expression. Small interfering RNA silencing of *TFIIA*γ markedly reduces levels of endogenous ATF4 protein and *Ocn* mRNA in osteoblastic cells. Overexpression of TFIIAγ increases levels of ATF4 protein. Finally, TFIIAγ significantly prevents ATF4 degradation. This study shows that a general transcription factor, TFIIAγ, facilitates osteoblast-specific gene expression through interactions with two important bone transcription factors ATF4 and Runx2.

Skeletal integrity requires a balance between bone-forming cells (osteoblasts) and bone-resorbing cells or osteoclasts. Imbalance between bone formation and resorption results in metabolic bone diseases such as osteoporosis. Multipotential mesenchymal cells proliferate and differentiate into osteoblasts that synthesize and deposit the mineralizing extracellular

[*]This work was supported by National Institutes of Health Grant DK072230 and Department of Defense Grant W81XWH-07-1-0160 (to G. X.). The costs of publication of this article were defrayed in part by the payment of page charges. This article must therefore be hereby marked "*advertisement*" in accordance with 18 U.S.C. Section 1734 solely to indicate this fact.

[S]The on-line version of this article (available at http://www.jbc.org) contains supplemental Fig. S1 and Fig S2.

1To whom correspondence should be addressed: Division of Hematology/Oncology, Dept of Medicine, University of Pittsburgh, Veterans Affairs Pittsburgh Healthcare System, Research and Development, 151-U, Rm. 2W-111, University Dr. C, Pittsburgh, PA 15240. Tel.: 412-688-6000 (Ext. 814459); Fax: 412- 688-6960; E-mail: xiaog@upmc.edu.

[2]The abbreviations used are: CREM, cAMP-response element modulator; TFIIAγ, transcription factor IIAγ; ChIP, chromatin immunoprecipitation; GST, glutathione *S*-transferase; WB, Western blot; IP, immunoprecipitation; FBS, fetal bovine serum; RT, reverse transcription; siRNA, small interfering RNA; aa, amino acids; CHX, cycloheximide; VDR, vitamin D receptor.

matrix of bone. Osteoblast activity is regulated by a number of growth factors and hormones, including bone morphogenetic proteins, insulin-like growth factor 1, basic fibroblast growth factor 2, parathyroid hormone, tumor necrosis factor-α, and extracellular matrix signals (1–9). Runx2 is a runt domain-containing transcription factor identified as a transcriptional activator of osteoblast differentiation and the master gene for bone development *in vitro* and *in vivo* (10–14). Runx2 knock-out mice die at birth and completely lack both skeletal ossification and mature osteoblasts (10,12). Runx2 haplo-insufficiency causes the skeletal disorder, cleidocranial dysplasia, a disease characterized by defective endochondral and intramembranous bone formation. Runx2 is expressed in mesenchymal condensations during early development at E11.5 and acts as an osteoblast differentiation factor (13).

ATF4 (activating transcription factor 4), also known as CREB2 (cAMP-response element-binding protein 2) (15) and Tax-responsive Enhancer Element B67 (TAXREB67) (16), is a member of the activating transcription factor cAMP-response element-binding protein family of leucine zipper factors that also includes cAMP-response element-binding protein, cAMP-response element modulator (CREM)[2] ATF1, ATF2, ATF3, and ATF4 (17–21). These proteins bind to DNA via their basic region and dimerize via their leucine domain to form a large variety of homodimers and/or heterodimers that allow the cell to coordinate signals from multiple pathways (17–21). An *in vivo* role for ATF4 in bone development was established using *Atf4*-deficient mice (22). ATF4 is required for expression of *osteocalcin (Ocn)* and *bone sialoprotein (Bsp)* as demonstrated by a dramatic reduction of their mRNAs in $Atf4^{-/-}$ bone (22). ATF4 activates *Ocn* transcription through direct binding to the OSE1 site of the *mOG2* promoter. In addition, ATF4 interacts with Runx2 in osteoblasts or when coexpressed in COS-7 cells. ATF4 and Runx2 cooperatively regulate *Ocn* transcription through interactions with OSE1 (osteoblast-specific element 1) and OSE2 (osteoblast-specific element 2, also known as nuclear matrix protein 2 or NMP2-binding site) sites in the promoter (23–25).

One of the most striking characteristics of ATF4 protein is its very short half-life (30–60 min) in many cell types (26). ATF4 is rapidly degraded via a ubiquitin/proteasomal pathway. This degradation requires the presence of the serine residue 219 in the context of DSG*XXX*S within the ATF4 molecule and its phosphorylation by an unknown kinase. This phosphorylation was shown to be required for subsequent recognition by the $SCF^{\beta TrCP}$ and degradation by the 26 S proteasome (27). Although *Atf4* mRNA is ubiquitously expressed, ATF4 protein preferentially accumulates in osteoblasts (28). This accumulation is explained by a selective reduction of proteasomal degradation in osteoblasts. Indeed, inhibition of the ubiquitin/proteasomal pathway by MG115, which blocks the N-terminal threonine in the active site of β-subunit of 26 S proteasomal complex (29,30), led to ATF4 accumulation and induced *Ocn* mRNA expression in non-osteoblastic cells (28). These observations suggest that modulation of ATF4 stability constitutes an important step to control its protein level and activity and, ultimately, osteoblast-specific gene expression and bone formation.

Transcription factor IIA (TFIIA) is a general transcription factor consisting of three subunits designated TFIIAα, TFIIAβ, and TFIIAγ (31). TFIIA interacts with and stabilizes TFIID (also known as TBP, TATA box-binding protein) to DNA and activates transcription (32,33). Although TFIIA was classified as a general transcription factor when it was first identified, more and more evidence shows that this elusive factor may play an important role in the regulation of tissue-specific gene expression via interactions with tissue- or cell type-specific transcription factors (34–36).

The *Ocn* promoter has been the major paradigm for unraveling the mechanisms mediating osteoblast-specific gene expression and defining a number of key transcription factors or

[S]The on-line version of this article (available at http://www.jbc.org) contains supplemental Fig. S1 and Fig S2.

cofactors (13,14,23–25,37–41). However, very few studies have focused on how tissue-specific transcription factors interface with general transcriptional initiation factors in osteoblasts. In this study, by using a combination of a yeast two-hybrid system and pulldown assays as well as functional assays, we show that TFIIAγ, the smallest subunit (12 kDa) of TFIIA (42), interacts with both Runx2 and ATF4. TFIIAγ delays ATF4 protein degradation and increases its activity. Together with ATF4 and Runx2, TFIIAγ enhances osteoblast-specific *Ocn* gene expression.

EXPERIMENTAL PROCEDURES

Reagents

Tissue culture media were purchased from Invitrogen and fetal bovine serum from HyClone (Logan, UT). Other reagents were obtained from the following sources: antibodies against TFIIA-α, TFIIA-γ, ATF4, Runx2, and horseradish peroxidase-conjugated mouse or goat IgG from Santa Cruz Biotechnology (Santa Cruz, CA), mouse monoclonal antibody against β-actin from Sigma, and GST antibody from Amersham Biosciences. All other chemicals were of analytical grade.

Cell Cultures

Mouse MC3T3-E1 subclone 4 (MC-4) cells were described previously (43,44) and maintained in ascorbic acid-free α-modified Eagle's medium, 10% fetal bovine serum (FBS), and 1% penicillin/streptomycin and were not used beyond passage 15. C2C12 myoblasts, a gift from Dr. Daniel Goldman (University of Michigan, Ann Arbor, MI), C3H10T1/2 fibroblasts (American Type Culture Collection), and 3T3-L1 mouse preadipocytes (American Type Culture Collection) were maintained in Dulbecco's modified Eagle's medium, 10% FBS. F9 teratocarcinoma cells (American Type Culture Collection) and rat ROS17/2.8 osteosarcoma cells (gift from Dr. Laurie McCauley, University of Michigan School of Dentistry) were grown in modified Eagle's medium, 10% FBS.

Yeast Two-hybrid Analysis

A yeast pLexA two-hybrid system (Clontech) was used to identify proteins that bind to mouse Runx2. A cDNA fragment encoding the aa-263–351 region of Runx2 was subcloned into the BamHI/XhoI sites of pLexA, creating an in-frame fusion with the DNA binding domain of the *LexA* gene that is controlled by the strong yeast *ADH1* promoter. The resultant plasmid pLexA-Runx2 (aa 263–351) was then transformed into a yeast reporter strain (YM4271), and the transformed cells (1×10^9) were mated for 24 h with cells (2.5×10^8) of a pretransformed two-hybrid library made from human brain cDNA. The resultant mating mixture was spread on 20 × 10-cm plates to select for expression of the *LEU2* and *lacZ* reporter genes. Approximately 2×10^6 colonies were screened. Sixty four positive colonies were isolated. The prey plasmids were extracted from the positive colonies and the cDNA inserts in the plasmids were amplified by PCR and sequenced. Of the 64 positive colonies, 5 are the full-length *TFIIA*γ cDNAs, and the rest contained 16 different cDNAs.

DNA Constructs and Transfection

p657mOG2-luc, p657m-OG2OSE1mt-luc, p657mOG2OSE2mt-luc, p657mOG2-(OSE1 + 2) mt-luc, p4OSE1-luc, p4OSE1mt-luc, p6OSE2-luc, p6OSE2mt-luc,pCMV/β-galactosidase, pCMV/ATF4,pCMV/Runx2, pCMV/FLAG-Runx2 and its deletion mutants (aa 1–330, aa 1–286, and aa-258), GST-Runx2 and GST-ATF4 fusion protein expression vectors were described previously (1,13,23,25,45). The full-length cDNA of human *TFIIA*-γ was cloned by an RT-PCR strategy using total RNA from human Saos2 osteoblastic cells as a template and specific primers (forward, 5′-ATG GCA TAT CAG TTA TAC AGA AA-3′, and reverse, 5′-

TTC TGT AGT ATT GGA GCC AGT A-3′). Digested PCR products were purified and subcloned into the NotI/BamHI sites of the pFLAG-5a expression vector (Sigma). Addition of a C-terminal FLAG sequence into the *TFIIA*-γ cDNA facilitates monitoring of expression levels and immunoprecipitation using M2 antibody (Sigma). GST-TFIIAγ fusion protein expression plasmid was constructed by subcloning the full-length *TFIIA*γ cDNA into the glutathione *S*-transferase gene fusion vector pGEX-4T-1 (Amersham Biosciences) in correct reading frame. The accuracy of DNA sequences was verified by automatic sequencing. The size of expressed proteins was confirmed by Western blot analysis using specific antibodies. For expression and functional studies, cells were plated on 35-mm dishes at a density of 5×10^4 cells/cm^2. After 24 h, cells were transfected with the indicated plasmid DNAs (0.01 μg of pRL-SV40, 0.25 μg of test luciferase reporter, and 1.0 μg of expression plasmids balanced as necessary with β-galactosidase expression plasmid such that the total DNA was constant) and Lipofectamine 2000 (Invitrogen) according to manufacturer's instructions. After 36 h, whole cell extracts were prepared and used for Western blot analysis or dual luciferase assay using the dual luciferase assay kit (Promega, Madison, WI) on a Veritas™ microplate luminometer (Turner Biosystem, Inc., Sunnyvale, CA). Firefly luciferase activity was normalized to *Renilla* luciferase activity for transfection efficiency.

RNA Isolation and Reverse Transcription (RT)

Total RNA was isolated using TRIzol reagent (Invitrogen) according to the manufacturer's protocol. RT was performed using 2 μg of denatured RNA and 100 pmol of random hexamers (Applied Biosystem, Foster, CA) in a total volume of 25 μl containing 12.5 units of MultiScribe reverse transcriptase (Applied Biosystem, Foster, CA) according to the manufacturer's instructions.

Regular PCR

Regular PCR was performed on a 2720 Thermal Cycler (Applied Biosystem, Foster, CA), using 2.5 μl of the cDNA (equivalent to 0.2 μg of RNA) and AmpliTaq DNA polymerase (Applied Biosystems, Foster City, CA) in a 25-μl reaction according to the manufacturer's instructions. The DNA sequences of primers used for PCR were as follows: mouse/rat *TFIIA*γ, 5′-ATG GCA TAT CAG TTA TAC AGA AAT ACA-3′ (forward), 5′-GGT ATT TTT ACC ATC ACA GGC T-3′(reverse); mouse/rat *Atf4*, 5′-ATG GCT TGG CCA GTG CCT CAG A-3′ (forward), 5′-GCT CTG GAG TGG AAG ACA GAA C-3′ (reverse); mouse/rat *Hprt*, 5′-GTT GAG AGA TCA TCT CCA CC-3′ (forward), 5′-AGC GAT GAT GAA CCA GGT TA-3′ (reverse). For all primers the amplification was performed as follows: initial denaturation at 95 °C for 30s followed by 31 cycles of 95 °C for 15 s, 60 °C for 30 s, 72 °C for 30 s and extension at 72 °C for 7 min. The amplified PCR products were run on a 1.2% agarose gel and visualized by ethidium bromide staining.

Quantitative Real Time PCR

Quantitative real time PCR was performed on an iCycler (Bio-Rad) using a SYBR® Green PCR core kit (Applied Biosystem, Foster, CA) and cDNA equivalent to 10 ng of RNA in a 50-μl reaction according to the manufacturer's instructions. The DNA sequences of primers used for real time PCR were as follows: mouse *Ocn*, 5′-TAG TGA ACA GAC TCC GGC GCT A-3′ (forward), 5′-TGT AGG CGG TCT TCA AGC CAT-3′ (reverse); mouse and rat *18 S rRNA*, 5′-CGT CTG CCC TAT CAA CTT TCG ATG GTA G-3′ (forward), 5′-GCC TGC TGC CTT CCT TGG ATG T-3′ (reverse); mouse and rat *TFIIA*γ, 5′-TGG GGA ACA GTC TTC AAG AGA GCC TT-3′ (forward); 5′-TTC CTG ACT CTC TGA GCC AAT GCT G-3′ (reverse); rat *Ocn*, 5′-TGG TGA ATA GAC TCC GGC GCT ACC T-3′ (forward), 5′-CCT GGA AGC CAA TGT GGT CCG-3′ (reverse); rat *Bsp*: 5′-GGC TGG AGA TGC AGA GGG CAA GGC-3′ (forward), 5′-TGG TGC TGG TGC CGT TGA CGA CCT-3′ (reverse); rat *Opn*, 5′-TGG TGA

ATA GAC TCC GGC GCT ACC T-3′ (forward), 5′-CCT GGA AGC CAA TGT GGT CCG-3′ (reverse). For all primers the amplification was performed as follows: initial denaturation at 95 °C for 10 min followed by 40 cycles of 95 °C for 15 s and 60 °C for 60 s. Melting curve analysis was used to confirm the specificity of the PCR products. Six samples were run for each primer set. The levels of mRNA were calculated by the Δ*CT* method (46). *Ocn*, *Bsp*, *TFIIA*γ, *osteopontin (Opn)*, and *Atf4* mRNAs were normalized to *18 S rRNA* mRNA.

Western Blot Analysis

Cells were washed with cold 1 × phosphate-buffered saline and lysed in 1 × Passive Buffer (Promega, Madison, WI) at room temperature for 20 min. Lysates were clarified by centrifugation (20 min, 13,000 × *g*, 4 °C). Protein concentrations were determined by the method developed by Bio-Rad. Twenty μg of total protein were fractionated on a 10% SDS-polyacrylamide gel and transferred onto nitrocellulose membranes (Schleicher & Schuell). The membrane was blocked in 5% nonfat milk in Tris-buffered saline/Tween 20 (TBST) buffer, probed with antibodies against TFIIA-γ (1:200), TFIIA-α (1:1000), ATF4 (1:1000), Runx2 (1:1000), Fra-1 (1:1000), GST (1:5000), or M2 (1:2000) followed by incubation with anti-goat-mouse or -rabbit antibodies conjugated with horseradish peroxidase (1:5000) and visualized using an enhanced chemiluminescence kit (Pierce). Finally, blots were stripped two times in buffer containing 65 mM Tris-Cl, pH 6.8, 2% SDS, and 0.7% (v/v) β-mercaptoethanol at 65 °C for 15 min and re-probed with β-actin antibody (1:5000) for normalization.

Immunoprecipitation

GST, GST-TFIIAγ, GST-ATF4, and GST-Runx2 fusion proteins were purified using the Bulk GST purification module kit (Amersham Biosciences) according the manufacturer's instructions. Whole cell extracts (500 μg), nuclear extracts (200 μg), or GST fusion proteins (1.0 μg) were pre-cleaned twice with 50 μl of protein A/G-agarose beads (Stratagene, La Jolla, CA) for 30 min followed by pelleting of beads. The protein A/G-agarose beads were blocked with 10 μg/ml bovine serum albumin in 1 × phosphate-buffered saline for 1 h before use to reduce nonspecific binding of proteins. Five μg of respective antibody was added and incubated for 2 h at 4 °C with gentle rocking. The immune complexes were collected by addition of 30 μl of protein A/G-agarose beads and incubation for 1 h at 4 °C followed by centrifugation. Precipitates were washed five times with 1 × washing buffer (20 mM HEPES, pH 7.6, 50mM KCl, 1mM dithiothreitol, 0.25% Nonidet P-40, 5 mM NaF, 1 mM EGTA, 5 mM $MgCl_2$, 0.25 mM phenylmethylsulfonyl fluoride), and the immunoprecipitated complexes were suspended in SDS sample buffer and analyzed by SDS-PAGE followed by Western blot analysis using the indicated antibodies.

ChIP Assays

ChIP assays were performed as described previously (41) using a protocol kindly provided by Dr. Dwight Towler (Washington University) (47). After sonication, the amount of chromatin was quantified using the PicoGreen double-stranded DNA quantitation assay (Molecular Probes) according to the manufacturer's instructions. The equivalent of 10 μg of DNA was used as starting material (input) in each ChIP reaction with 2 μg of the appropriate antibody (TFIIAγ, or control rabbit IgG). Fractions of the purified ChIP DNA (5%) or inputs (0.02–0.05%) were used for PCR analysis. The reaction was performed with AmpliTaq Gold DNA polymerase (Applied Biosystems) for 35 cycles of 60 s at 95 °C, 90 s at 58 °C, and 120 s at 68 °C. PCR primer pairs were generated to detect DNA segments located near the Runx2-binding site at −137/−131 (primers P1 and P2), ATF4-binding site at −55/−48 (primers P3 and P4) in mouse *osteocalcin* gene 2 (*mOG2*) proximal promoter, or the Runx2-binding site located between −370 and −42 in the proximal mouse *Runx2* promoter region (primers P5 and P6) (48), and the *mOG2* gene region (+177/+311) (primers P7 and P8) (see Fig. 2*A* and Table 1).

The PCR products were separated on 3% agarose gels and visualized with ultraviolet light. All ChIP assays were repeated at least three times.

siRNA

ROS17/2.8 osteoblast-like cells, which contain high levels of TFIIAγ protein, were transfected with mouse *TFIIA*γ siRNA kit (Santa Cruz Biotechnology) or negative control siRNA(low GC, catalog number 12935-200, Invitrogen) using Lipofectamine 2000 (Invitrogen) according the manufacturer's instruction. After 36 h, total RNA was harvested for quantitative real time RT-PCR analysis for *TFIIA*γ, *Ocn, Bsp, Opn (osteopontin)*, and *Atf4* mRNAs. A second set of mouse *TFIIA*γ siRNAs (sense, AUG ACA ACA CUG UGC UAU AUU; anti-sense, UAU AGC ACA GUG UUG UCA UUU) was designed in the project laboratory and used to confirm the results using the first set of *TFIIA*γ siRNA.

Statistical Analysis

Results were expressed as means ± S.D. Students' *t* test was used to test for differences between two groups. Differences with a $p < 0.05$ was considered as statistically significant.

RESULTS

TFIIAγ Interacts with Runx2 and ATF4

A yeast pLexA two-hybrid system (Clontech) was used to identify proteins that bind to mouse Runx2. cDNA fragments encoding several C-terminal regions of Runx2 were subcloned into the BamHI/XhoI sites of pLexA, creating in-frame fusions with the DNA binding domain of the *LexA* gene that is controlled by the strong yeast *ADH1* promoter. Preliminary experiments using relatively larger regions of Runx2 (aa 232–391, aa 232–428, and aa 232–517) as baits were not successful because of their ability to autoactivate the *lacZ* reporter gene in yeast. In contrast, by using the aa 263–351 region of Runx2 as a bait, we identified TFIIAγ, a general transcriptional factor involved in the initiation step of eukaryotic transcription, as a Runx2-interacting factor. A diagram and a picture of a positive colony are shown in Fig. S1.

To verify the TFIIAγ-Runx2 interaction identified by yeast two-hybrid system, we conducted pulldown assays. COS-7 cells were transiently transfected with expression vectors for FLAG-TFIIAγ, Runx2, and ATF4 (a recently identified Runx2-interacting factor). After 36 h, whole cell extracts were prepared for immunoprecipitation (IP) assay using a TFIIAγ antibody followed by Western blot analysis for Runx2 and ATF4. As seen in Fig. 1*A* (*lane 2*), Runx2 protein was present in a TFIIAγ antibody immunoprecipitate. Interestingly, anti-TFIIAγ antibody also immunoprecipitated ATF4. Reciprocal IPs showed that both Runx2 and ATF4 antibodies immunoprecipitated the FLAG-tagged TFIIAγ (Fig. 1*A*, *lanes 4* and *6*). To determine whether TFIIAγ can interact with Runx2 and ATF4 in osteoblasts, nuclear extracts from ROS17/2.8 cells that express high levels of Runx2, ATF4, and TFIIAγ were immunoprecipitated with anti-TFIIAγ antibody followed by Western blot analysis for Runx2, ATF4, or Fra-1 (a member of AP1 family). Results show that both Runx2 and ATF4 but not Fra-1 proteins were present in anti-TFIIAγ immunoprecipitates (Fig. 1*B*, *lane 2*). Reciprocal IPs showed that antibodies against Runx2 or ATF4 but not Fra-1 immunoprecipitated TFIIAγ in ROS17/2.8 cells (Fig. 1*B*, *lanes 4*, *6*, and *8*). Normal control IgG failed to significantly pull down Runx2, ATF4, or TFIIAγ in either COS-7 cells or osteoblasts. Taken together, these studies confirm that TFIIAγ interacts with Runx2 and ATF4 in osteoblasts or when coexpressed in COS-7 cells.

Although Runx2 and ATF4 interact in osteoblasts, IP assays using purified GST fusion proteins failed to show a direct physical interaction between ATF4 and Runx2 (25), suggesting that accessory factors may be involved in their interactions. To determine whether TFIIAγ can

directly interact with Runx2 or ATF4 in the absence of other nuclear proteins, we mixed GST or GST-TFIIAγ with GST-ATF4 or GST-Runx2 fusion proteins purified from *Escherichia coli*, followed by IP and Western blot analysis. As shown in Fig. 1*C*, both GST-Runx2 and GST-ATF4 proteins mixed with GST-TFIIAγ were immunoprecipitated by anti-TFIIAγ antibody (*lanes 1* and *2*). Anti-Runx2 or anti-ATF4 antibody was unable to immunoprecipitate GST protein mixed with GST-Runx2 (Fig. 1*C*, *lane 3*) or GST-ATF4 (*lane 4*). Reciprocal IPs show that GST-TFIIAγ was immunoprecipitated by both anti-Runx2 or anti-ATF4 antibodies (Fig. 1*C*, *lanes 6* and *7*) but not by normal control IgG (*lane 5*). These results demonstrate that TFIIAγ directly binds to both Runx2 and ATF4.

As a first step to identify the TFIIAγ-binding domain, FLAG-Runx2 deletion mutant expression vectors (wild type aa 1–528, aa 1–330, aa 1–286, and aa 1–258) were transfected into COS-7 cells because of the high transfection efficiency. Nuclear extracts were prepared 36 h later, mixed with equal amounts of nuclear extracts of ROS17/2.8 (which contain large amounts of endogenous TFIIAγ), and immunoprecipitated using anti-TFIIAγ antibody followed by Western blot analysis for Runx2 (M2 antibody). As shown in Fig. 1*D*, deletion of Runx2 from aa 528 to aa 286 did not reduce TFIIAγ binding. However, further deletion from aa 286 to aa 258 completely abrogated TFIIAγ-Runx2 complex formation. These data clearly demonstrate the following: (i) endogenous TFIIAγ can interact with overexpressed FLAG-Runx2 proteins *in vitro*; and (ii) the aa 258–286 region of Runx2 is required for TFIIAγ binding. Interestingly, this same region is required for ATF4-Runx2 interactions (25).

To determine whether, in intact cells, TFIIAγ is associated with the endogenous *osteocalcin* gene 2 (*mOG2*) promoter region that has been shown to bind Runx2 and ATF4, we performed the chromatin immunoprecipitation (ChIP) assay using MC3T3-E1 (clone MC-4) preosteoblast cells. After shearing, soluble chromatin was immunoprecipitated with either an antibody against TFIIAγ or control IgG. The positions and sequences of primers used for PCR analysis of ChIP DNAs are shown in Fig. 2*A* and Table 1. As shown in Fig. 2*B*, the PCR bands amplified with primers P1/P2 and P3/P4 and corresponding to ChIP DNAs immunoprecipitated with TFIIAγ antibody revealed that TFIIAγ specifically interacts with chromatin fragments of the proximal *mOG2* promoter that contain Runx2- or ATF4-binding sites. Furthermore, TFIIAγ antibody also immunoprecipitated a Runx2-binding site-containing chromatin fragment of the proximal *Runx2* promoter (primers P5/P6). In contrast, TFIIAγ antibody failed to immunoprecipitate a chromatin fragment of *mOG2* gene that contains no Runx2- or ATF4-binding sites (primers P7/P8). Taken together, these data show that TFIIAγ is recruited to a chromatin fragment of the *mOG2* promoter that was previously demonstrated to be bound by Runx2 and ATF4 in osteoblasts (13,22).

TFIIAγ Increases ATF4 but Not Runx2-dependent Transcriptional Activity

To determine whether *TFIIA*γ increases Runx2- and ATF4-dependent transcriptional activity, we measured the ability of TFIIAγ to stimulate transcription of p6OSE2-luc, a reporter plasmid containing 6 copies of the Runx2-binding element OSE2 upstream of a minimal 34-bp *mOG2* promoter (13,43,49) or p4OSE1-luc, a reporter plasmid that contains four copies of OSE1 (a specific ATF4-binding element) upstream of a minimal 34-bp *mOG2* promoter (22, 25). For these studies, we used C3H10T1/2 fibroblasts because they contain undetectable levels of both endogenous Runx2 and ATF4 proteins (28,49). As shown in Fig. 3*A*, as expected, Runx2 alone increased OSE2 transcriptional activity by 11-fold. This stimulation was abolished in the 6OSE2mt-luc in which the OSE2 core sequence was mutated (25) (Fig. 3*B*). Although we have shown above that TFIIAγ interacts with Runx2, TFIIAγ transfection did not activate basal or Runx2-dependent OSE2 transcription (Fig. 3*A*). As shown in Fig. 3*C*, ATF4 activated OSE1 activity about 2-fold ($p < 0.01$, β-galactosidase *versus* ATF4). Although TFIIAγ alone was unable to activate OSE1 activity, unexpectedly, when coexpressed with

ATF4, it dramatically increased OSE1 activity 5-fold above ATF4 alone. This stimulation was abolished in 4OSE1mt-luc, in which the OSE1 core sequence was mutated from TTACATCA to TTAGTACA in the reporter plasmid (45) (Fig. 3*D*). Note: TFIIAγ, Runx2, or ATF4 failed to activate a minimal 34-bp *mOG2* promoter that contains a TATA box (23,50) (Fig. 3*E*). Fig. 3*F* shows that TFIIAγ activated ATF4 transcription activity in a dose-dependent manner in C3H10T1/2 cells. TFIIAγ similarly stimulated ATF4-directed OSE1 activity in C2C12 myoblasts (3-fold) and COS-7 cells (4.3-fold) (Fig. 3, *G* and *H*).

TFIIAγ Expression in Different Cell Lines

The levels of *TFIIA*γ mRNAs and proteins were determined in different cell lines by RT-PCR and Western blot analysis, respectively. As shown in Fig. 4, Western blot analysis shows that TFIIAγ protein was expressed at high levels in osteoblastic cells (MC-4 cells and ROS17/2.8), C3H10T1/2 fibroblasts, and L1 preadipocytes. In contrast, levels of TFIIAγ protein were undetectable in F9 teratocarcinoma cells and COS-7 (transformed African green monkey kidney fibroblasts). Interestingly, *TFIIA*γ mRNA was ubiquitously expressed in these cell lines. In addition, TFIIAα proteins were present in all these cell lines except for ROS17/2.8 cells, which contain a low level of TFIIAα protein.

TFIIAγ Stimulation of Endogenous Ocn mRNA Expression and the 657-bp mOG2 Promoter Activity Is Dependent upon the Presence of ATF4 and Runx2

ATF4 is an osteoblast-enriched protein that is required for late osteoblast differentiation (*i.e. Ocn* and *Bsp* mRNA expression) and bone formation *in vivo*. Our recent study demonstrated that ATF4 activation of *mOG2* promoter activity and *Ocn* mRNA expression was dependent upon the presence of Runx2 via a mechanism involving protein-protein interactions (25). To determine the effects of TFIIAγ on endogenous *Ocn* mRNA expression, C3H10T1/2 cells were transiently transfected with expression vectors for β-galactosidase, TFIIAγ, ATF4, Runx2, ATF4/Runx2, TFIIAγ/Runx2, TFIIAγ/ATF4, and ATF4/Runx2/TFIIAγ. After 36 h, cells were harvested for RNA preparation and quantitative real time RTPCR detection of *Ocn* mRNA. As shown in Fig. 5*A*, consistent with its role as a master gene of osteoblast differentiation, Runx2 alone increased endogenous *Ocn* expression by 3.3-fold ($p < 0.01$; β-galactosidase *versus* Runx2). TFIIAγ alone, ATF4 alone, and TFIIAγ/ATF4 were all not sufficient for activation of endogenous *Ocn* mRNA expression. TFIIAγ alone did not enhance Runx2-dependent *Ocn* expression. As demonstrated previously (25), ATF4 dramatically stimulated Runx2-dependent *Ocn* mRNA expression by 10-fold ($p < 0.01$, Runx2 *versus* Runx2/ATF4). Importantly, TFIIAγ further augmented *Ocn* mRNA expression 4.2-fold in the presence of ATF4 and Runx2 ($p < 0.01$, ATF4/Runx2 *versus* ATF4/Runx2/TFIIAγ). TFIIAγ similarly enhanced ATF4/Runx2-dependent 657-bp *mOG2* promoter activity in C3H0T1/2 cells (3.6-fold) (Fig. 5*B*) ($p < 0.01$, ATF4/Runx2 *versus* ATF4/Runx2/TFIIAγ). This stimulation was completely abolished by point mutations in the OSE1 and/or OSE2 core sequences.

Silencing of TFIIAγ Markedly Reduces Levels of Endogenous Ocn and Bsp mRNAs and ATF4 Protein in Osteoblasts

To determine whether TFIIAγ is required for the endogenous *Ocn* mRNA expression in osteoblasts, we knocked down the endogenous *TFIIA*γ transcripts by siRNA. ROS17/2.8 osteoblast-like cells, which express high levels of *TFIIA*γ and *Ocn* and *Bsp* mRNAs, were transiently transfected with *TFIIA*γ siRNA reagent from Santa Cruz Biotechnology according to the manufacturer's instructions. This siRNA is a pool of three specific 20–25-nucleotide siRNA targeting both mouse and rat *TFIIA*γ. As shown in Fig. 6*A*, quantitative real time RT-PCR analysis showed that levels of *TFIIA*γ mRNA were efficiently reduced by *TFIIA*γ siRNA in a dose-dependent manner. The level of *Ocn* mRNA was reduced greater than 50% by *TFIIA*γ siRNA ($p < 0.01$, control *versus TFIIA*γ siRNA). Interestingly, *Bsp* mRNA, another

ATF4 downstream target gene (22), was also reduced by 50% ($p < 0.01$, control *versus* *TFIIA*γ siRNA). This inhibition was specific because levels of *Opn* and *Atf4* mRNAs were not reduced by *TFIIA*γ siRNA. In contrast, as shown in Fig. 6*B*, levels of all these mRNAs were not reduced by the negative control siRNA (Invitrogen). Although *Atf4* mRNA was not altered by *TFIIA*γ siRNA, the level of endogenous ATF4 protein was significantly reduced by silencing *TFIIA*γ in osteoblasts (Fig. 6*C*). Similar results were obtained when a different set of TFIIAγ siRNA was used (Fig. S2).

Overexpression of TFIIAγ Increases the Levels of ATF4 Protein

The above studies clearly demonstrated that TFIIAγ increased ATF4-dependent transcription activity and *Ocn* gene expression probably by targeting ATF4 protein. To further study the mechanism of this regulation, we determined the effect of TFIIAγ overexpression on the levels of ATF4 protein. C3H10T1/2 cells, which express undetectable level of endogenous ATF4 protein (28), were transiently transfected with 1.0 μg of ATF4 expression plasmid and increasing amounts of TFIIAγ expression plasmid (0, 0.5, 1, and 2 μg). After 36 h, cells were harvested for Western blot analysis. As shown in Fig. 7*A*, overexpression of TFIIAμ in C3H10T1/2 cells increased the levels of ATF4 protein in a dose-dependent manner. This increase in ATF4 protein was specific because levels of Runx2 were not altered by TFIIAγ. TFIIAγ similarly elevated levels of ATF4 protein in COS-7 cells (Fig. 7*B*). Next, we determined if TFIIAγ could increase the levels of endogenous ATF4 proteins in osteoblasts. ROS17/2.8 cells were transiently transfected with indicated amount of TFIIAγ expression vector. Western blot analysis shows that TFIIAγ dose-dependently increased levels of endogenous ATF4 protein in ROS17/2.8 cells (Fig. 7*C*). Similar results were obtained in MC-4 cells (Fig. 7*D*). Interestingly, overexpression of TFIIAγ did not increase the levels of *Atf4* mRNA in all these cells examined (*bottom*, Fig. 7, *A–D*). Taken collectively, TFIIAγ markedly increased levels of ATF4 proteins in osteoblasts and non-osteoblasts.

TFIIAγ Increases ATF4 Protein Stability

Lassot *et al.* (51) recently showed that acetylase p300 markedly increased the levels of ATF4 protein and ATF4-dependent transcriptional activity by inhibiting ATF4 protein degradation via a proteasomal ubiquitin pathway. As an initial step to determine whether TFIIAγ alters ATF4 protein stability, C3H10T1/2 cells were transiently transfected with ATF4 expression vector in the presence of β-galactosidase, TFIIAγ, or Runx2 expression vectors. After 36 h, cells were treated with 50 μg/ml of protein synthesis inhibitor cycloheximide (CHX) (*i.e.* to completely block *de novo* protein synthesis) and harvested at different time points of CHX addition (0, 0.5, 1, and 3 h) followed by Western blot analysis for ATF4 and Runx2. This technique has been widely used to study protein stability (51). As shown in Fig. 8*A*, in the absence of TFIIAγ overexpression, ATF4 protein was rapidly degraded and almost undetectable on Western blot by 3 h after CHX addition, which is consistent with a previous study (51). However, overexpression of TFIIAγ greatly delayed the degradation process with the levels of ATF4 protein only slightly reduced by 3 h after CHX addition. In contrast, levels of Runx2 protein were not affected by TFIIAγ (Fig. 8*B*).

DISCUSSION

This study identifies TFIIAγ as a bridging molecule between Runx2, ATF4, and the transcription machinery in osteoblasts. Although Runx2 and ATF4 interact in osteoblasts or when coexpressed in COS-7 cells, IPs using purified GST fusion proteins were unable to demonstrate a direct physical interaction between ATF4 and Runx2 (25). Thus, accessory factors are likely involved in bridging these two molecules. Several lines of evidence support that TFIIAγ may be a factor linking Runx2 and ATF4. (i) TFIIAγ forms complexes with both Runx2 and ATF4 in osteoblasts and when coexpressed in COS-7 cells. (ii) The same region

of Runx2 (*i.e.* Aa 258 –286) is required for both TFIIAγ-Runx2 and ATF4-Runx2 interactions. (iii) Purified GST-TFIIAγ fusion protein directly binds to both purified GST-Runx2 and GST-ATF4 fusion proteins. (iv) Overexpression of TFIIAγ in 10T1/2 cells dramatically enhances endogenous *Ocn* gene expression and the 657-bp *mOG2* promoter activity in the presence of ATF4 and Runx2. (v) siRNA knockdown of *TFIIA*γ mRNA markedly reduces osteoblast-specific *Ocn* and *Bsp* expression.

Accumulating evidence establishes that ubiquitin-proteasome pathways control osteoblast differentiation and bone formation. For example, the proteasome inhibitors epoxomicin and proteasome inhibitor-1, when administered systemically to mice, strongly stimulated bone volume and bone formation rates by greater than 70% after only 5 days of treatment (52). Although the mechanism of this regulation remains unclear, critical bone transcription factors seem to be targets for the ubiquitin-proteasomal pathway. Zhao and co-workers (52,53) recently showed that Smurf1, an E3 ubiquitin-protein isopeptide ligase, accelerated Runx2 ubiquitin-proteasomal degradation and inhibited osteoblast differentiation and bone formation *in vitro* and *in vivo*. Although *Atf4* mRNA is ubiquitously expressed, in most cells ATF4 proteins are rapidly degraded via the ubiquitin-proteasome pathway with a half-life of 30–60 min. However, this degradation pathway is less active in osteoblasts, thereby allowing ATF4 accumulation (28). Indeed, inhibition of the ubiquitin/proteasomal pathway by MG115, which blocks the N-terminal threonine in the active site of β-subunit of 26 S proteasomal complex (29,30), led to ATF4 accumulation and induced *Ocn* mRNA expression in non-osteoblastic cells (28). Similarly, silencing of β-*TrCP1*, an E3 ubiquitin-protein isopeptide ligase that interacts with ATF4, by RNA interference, resulted in ATF4 accumulation and increased *Ocn* expression. Thus, ATF4 is a major target of the uquibitin-proteasome pathway, and modulation of ATF4 stability may play a critical role in the regulation of osteoblast-specific gene expression. Because β-*TrCP1* is present in osteoblasts (28), other factor(s) must be present in these cells to protect ATF4 from the proteasomal degradation that occurs in other cell types. Experiments from this study show that overexpression of TFIIAγ dose-dependently increases ATF4 protein in osteoblasts (ROS17/2.8 and MC-4 cells) and non-osteoblasts (C3H10T1/2 and COS-7 cells) without altering *Atf4* mRNA. Experiments using the protein synthesis inhibitor CHX further demonstrate that TFIIAγ greatly inhibits ATF4 degradation. TFIIAγ siRNA decreases ATF4 stability in osteoblasts. Lassot *et al.* (51) recently found that ATF4 is similarly stabilized by cofactor p300, a histone acetyltransferase. p300 inhibits ATF4 ubiquitination and degradation through interaction with the ATF4 N terminus. Interestingly, this stabilization does not require either the acetyltransferase activity of p300 or the serine residue 219 in the context of DSG*XXX*S within ATF4 molecule that is known to be required for ATF4 degradation via the $SCF^{\beta TrCP}$ and the 26 S proteasome (51).

TFIIAγ stimulation of *Ocn* gene transcription is dependent on the presence of both ATF4 and Runx2. As a master regulator of osteoblast differentiation, Runx2 alone is sufficient to activate expression of many osteoblast-specific genes, including *Ocn* and *Bsp*, by direct binding to their promoters (13). In contrast, although ATF4 directly binds to the OSE1 site of the mouse *Ocn* gene and activates OSE1, it alone is not sufficient for activation of the endogenous *Ocn* gene or the 657-bp *mOG2* promoter which contains sufficient information for the bone-specific expression of *Ocn in vivo* (54). Instead, ATF4 stimulation of *Ocn* is dependent on the presence of Runx2 as demonstrated by our recent study (25). ATF4 interacts with Runx2 and activates Runx2-dependent transcriptional activity. A recent study shows that SATB2, a nuclear matrix protein that directly interacts with both ATF4 and Runx2, activates osteoblast differentiation and controls craniofacial patterning *in vivo* (55). This study shows that although TFIIAγ interacts with Runx2, it does not directly activate Runx2. Like ATF4, TFIIAγ alone is not sufficient to activate transcription from either the *Ocn* gene or the 657-bp *mOG2* promoter. In fact, even TFIIAγ and ATF4 together are not sufficient for *Ocn* gene expression without the

presence of Runx2 (Fig. 5). However, in the presence of both ATF4 and Runx2, TFIIAγ greatly activates *Ocn* gene expression.

General transcription factors were originally defined as such because they were thought to be universally required for transcription. In eukaryotic cells, initiation of transcription is a complex process, which requires RNA polymerase II and many other basal transcription factors and/or cofactors, including TFIIA, TFIIB, TFIID (TBP or TATA box-binding protein), TFIIE, TFIIF, and TFIIH (56–59). Binding of TBP to the TATA box is the first step, which is regulated by TFIIA. TFIIA enhances transcription by interacting with TBP and stabilizing its binding to DNA (32,33). More and more evidence shows that general transcription factors play unique roles in the regulation of tissue-specific gene expression under physiological and pathological conditions. For example, the androgen receptor, via its N-terminal AF1 domain, interacts with basal transcription factors TBP and TFIIF and activates tissue-specific transcription in target tissues and cells (60). Likewise, $TAFII_{17}$ (a component of the TFIID complex), via specific protein-protein interactions with the vitamin D receptor (VDR), increases osteoclast formation from osteoclast precursors in response to 1,25-dihydroxyvitamin D3 in patients with Paget disease (61). In osteoblasts, bone transcription factors such as Runx2 and ATF4 directly bind to specific DNA sequences in their target gene promoters (*i.e.* OSE2 or NMP2 and OSE1, respectively) and activate osteoblast-specific gene expression, osteoblast differentiation, and bone formation (1,10–14,24,43). Obviously, cooperative interactions between osteoblast-specific transcription factors and basal (general) transcriptional machinery are essential for achieving maximal transcription of osteoblast-specific genes. However, little is known about these interactions. Experiments from this study demonstrate that TFIIAγ, which is expressed at high level in osteoblasts, facilitates osteoblast-specific gene expression via two mechanisms. 1) TFIIAγ stabilizes ATF4 and increases the levels of ATF4 proteins. The increased levels of ATF4 further activate Runx2 activity and *Ocn* transcription (25). 2) Through its ability to directly interact with both ATF4 and Runx2, TFIIAγ could recruit these two critical bone transcription factors to the basal transcriptional machinery and greatly enhance osteoblast-specific gene expression. In support of our observation, Guo and Stein (62) showed that Yin Yang-1 (YY1) regulates vitamin D enhancement of *Ocn* gene transcription by interfering with interactions of the VDR with both the VDR element and TFIIB. TFIIB interacts with both VDR and YY1 (63). Likewise, Newberry *et al.* (64) showed that TFIIF (RAP74 and RAP30) mediates Msx2 (a homeobox transcription factor required for craniofacial development) inhibition of *Ocn* promoter activity. Finally, a recent study showed that TFIIB could directly bind to the transactivation domain of Osterix, another important osteoblast transcription factor (65).

TFIIA consists of three subunits designated TFIIAα, TFIIAβ, and TFIIAγ. TFIIAα and TFIIAβ are produced by a specific proteolytic cleavage of the αβ polypeptide that is encoded by *TFIIA-L* (31,33). TFIIAγ is the smallest subunit with a molecular mass of 12 kDa (42). Although it is encoded by a distinct gene (*TFIIAγ*), TFIIAγ shares a high degree of homology with TFIIAα and TFIIAβ. Interestingly, TFIIAα activates testis-specific gene expression via interactions with a tissue-specific partner, ACT (activator of CREM in testis) and CREM (34). Likewise, TFIIAα enhances human T-cell lymphotropic virus type 1 gene activation through interactions with the Tax protein, a factor associated with adult enhances human T-cell lymphotropic virus type 1 (*HTLV-1*) (35,66). It remains to be determined whether TFIIAα and TFIIAβ can also interact with ATF4 and Runx2 and similarly activate osteoblast-specific gene expression.

It should be noted that although TFIIAγ belongs to the family of general transcription factors, its expression seems to show some tissue or cell specificity. Osteoblastic cells (MC-4 cells and ROS17/2.8), C3H10T1/2 fibroblasts, and L1 preadipocytes express high levels of TFIIAγ

proteins. In contrast, the levels of TFIIAγ protein were undetectable in F9 teratocarcinoma cells and COS-7 on Western blots. The meaning of this observation remains unknown.

These findings suggest that TFIIAγ is a critical factor regulating ATF4 stability and functions as a molecular linker between ATF4 and Runx2 and the basal transcriptional machinery. TFIIAγ may play a unique role in the regulation of osteoblast-specific gene expression and ultimately osteoblast differentiation and bone formation. A working model is proposed in Fig. 9, which summarizes the role of TFIIAγ in osteoblast-specific *mOG2* gene expression. Future study aimed at identifying factors that affect levels and activity of TFIIAγ will allow us to address the functional significance of TFIIAγ in osteoblast function in greater detail.

Acknowledgment

We thank Drs. G. David Roodman (University of Pittsburgh) and Renny T. Franceschi (University of Michigan) for critical reading of the manuscript.

REFERENCES

1. Yang S, Wei D, Wang D, Phimphilai M, Krebsbach PH, Franceschi RT. J. Bone Miner. Res 2003;18:705–715. [PubMed: 12674331]
2. Xiao G, Jiang D, Gopalakrishnan R, Franceschi RT. J. Biol. Chem 2002;277:36181–36187. [PubMed: 12110689]
3. Gilbert L, He X, Farmer P, Rubin J, Drissi H, van Wijnen AJ, Lian JB, Stein GS, Nanes MS. J. Biol. Chem 2002;277:2695–2701. [PubMed: 11723115]
4. Krishnan V, Moore TL, Ma YL, Helvering LM, Frolik CA, Valasek KM, Ducy P, Geiser AG. Mol. Endocrinol 2003;17:423–435. [PubMed: 12554794]
5. Xiao G, Gopalakrishnan R, Jiang D, Reith E, Benson MD, Franceschi RT. J. Bone Miner. Res 2002;17:101–110. [PubMed: 11771655]
6. Zhang X, Sobue T, Hurley MM. Biochem. Biophys. Res. Commun 2002;290:526–531. [PubMed: 11779203]
7. Hurley MM, Tetradis S, Huang YF, Hock J, Kream BE, Raisz LG, Sabbieti MG. J. Bone Miner. Res 1999;14:776–783. [PubMed: 10320526]
8. Montero A, Okada Y, Tomita M, Ito M, Tsurukami H, Nakamura T, Doetschman T, Coffin JD, Hurley MM. J. Clin. Investig 2000;105:1085–1093. [PubMed: 10772653]
9. Yakar S, Rosen CJ, Beamer WG, Ackert-Bicknell CL, Wu Y, Liu JL, Ooi GT, Setser J, Frystyk J, Boisclair YR, LeRoith D. J. Clin. Investig 2002;110:771–781. [PubMed: 12235108]
10. Komori T, Yagi H, Nomura S, Yamaguchi A, Sasaki K, Deguchi K, Shimizu Y, Bronson RT, Gao YH, Inada M, Sato M, Okamoto R, Kitamura Y, Yoshiki S, Kishimoto T. Cell 1997;89:755–764. [PubMed: 9182763]
11. Otto F, Thornell AP, Crompton T, Denzel A, Gilmour KC, Rosewell IR, Stamp GW, Beddington RS, Mundlos S, Olsen BR, Selby PB, Owen MJ. Cell 1997;89:765–771. [PubMed: 9182764]
12. Mundlos S, Otto F, Mundlos C, Mulliken JB, Aylsworth AS, Albright S, Lindhout D, Cole WG, Henn W, Knoll JH, Owen MJ, Mertelsmann R, Zabel BU, Olsen BR. Cell 1997;89:773–779. [PubMed: 9182765]
13. Ducy P, Zhang R, Geoffroy V, Ridall AL, Karsenty G. Cell 1997;89:747–754. [PubMed: 9182762]
14. Banerjee C, McCabe LR, Choi JY, Hiebert SW, Stein JL, Stein GS, Lian JB. J. Cell. Biochem 1997;66:1–8. [PubMed: 9215522]
15. Karpinski BA, Morle GD, Huggenvik J, Uhler MD, Leiden JM. Proc. Natl. Acad. Sci. U. S. A 1992;89:4820–4824. [PubMed: 1534408]
16. Tsujimoto A, Nyunoya H, Morita T, Sato T, Shimotohno K. J. Virol 1991;65:1420–1426. [PubMed: 1847461]
17. Brindle PK, Montminy MR. Curr. Opin. Genet. Dev 1992;2:199–204. [PubMed: 1386267]

18. Hai T, Wolfgang CD, Marsee DK, Allen AE, Sivaprasad U. Gene Expr 1999;7:321–335. [PubMed: 10440233]
19. Meyer TE, Habener JF. Endocr. Rev 1993;14:269–290. [PubMed: 8319595]
20. Sassone-Corsi P. EMBO J 1994;13:4717–4728. [PubMed: 7957042]
21. Ziff EB. Trends Genet 1990;6:69–72. [PubMed: 2158162]
22. Yang X, Matsuda K, Bialek P, Jacquot S, Masuoka HC, Schinke T, Li L, Brancorsini S, Sassone-Corsi P, Townes TM, Hanauer A, Karsenty G. Cell 2004;117:387–398. [PubMed: 15109498]
23. Ducy P, Karsenty G. Mol. Cell. Biol 1995;15:1858–1869. [PubMed: 7891679]
24. Merriman HL, van Wijnen AJ, Hiebert S, Bidwell JP, Fey E, Lian J, Stein J, Stein GS. Biochemistry 1995;34:13125–13132. [PubMed: 7548073]
25. Xiao G, Jiang D, Ge C, Zhao Z, Lai Y, Boules H, Phimphilai M, Yang X, Karsenty G, Franceschi RT. J. Biol. Chem 2005;280:30689–30696. [PubMed: 16000305]
26. Hai T, Hartman MG. Gene (Amst.) 2001;273:1–11. [PubMed: 11483355]
27. Lassot I, Segeral E, Berlioz-Torrent C, Durand H, Groussin L, Hai T, Benarous R, Margottin-Goguet F. Mol. Cell. Biol 2001;21:2192–2202. [PubMed: 11238952]
28. Yang X, Karsenty G. J. Biol. Chem 2004;279:47109–47114. [PubMed: 15377660]
29. Lee DH, Goldberg AL. J. Biol. Chem 1996;271:27280–27284. [PubMed: 8910302]
30. Rock KL, Gramm C, Rothstein L, Clark K, Stein R, Dick L, Hwang D, Goldberg AL. Cell 1994;78:761–771. [PubMed: 8087844]
31. Hoiby T, Zhou H, Mitsiou DJ, Stunnenberg HG. Biochim. Biophys. Acta 2007;1769:429–436. [PubMed: 17560669]
32. Zhou H, Spicuglia S, Hsieh JJ, Mitsiou DJ, Hoiby T, Veenstra GJ, Korsmeyer SJ, Stunnenberg HG. Mol. Cell. Biol 2006;26:2728–2735. [PubMed: 16537915]
33. Hoiby T, Mitsiou DJ, Zhou H, Erdjument-Bromage H, Tempst P, Stunnenberg HG. EMBO J 2004;23:3083–3091. [PubMed: 15257296]
34. De Cesare D, Fimia GM, Brancorsini S, Parvinen M, Sassone-Corsi P. Mol. Endocrinol 2003;17:2554–2565. [PubMed: 14512522]
35. Duvall JF, Kashanchi F, Cvekl A, Radonovich MF, Piras G, Brady JN. J. Virol 1995;69:5077–5086. [PubMed: 7609077]
36. Zhao C, Irie N, Takada Y, Shimoda K, Miyamoto T, Nishiwaki T, Suda T, Matsuo K. Cell Metab 2006;4:111–121. [PubMed: 16890539]
37. Geoffroy V, Ducy P, Karsenty G. J. Biol. Chem 1995;270:30973–30979. [PubMed: 8537354]
38. Stein GS, Lian JB, van Wijnen AJ, Stein JL. Mol. Biol. Rep 1997;24:185–196. [PubMed: 9291092]
39. Banerjee C, Hiebert SW, Stein JL, Lian JB, Stein GS. Proc. Natl. Acad. Sci. U. S. A 1996;93:4968–4973. [PubMed: 8643513]
40. Lian JB, Stein GS. Curr. Pharm. Des 2003;9:2677–2685. [PubMed: 14529540]
41. Roca H, Phimphilai M, Gopalakrishnan R, Xiao G, Franceschi RT. J. Biol. Chem 2005;280:30845–30855. [PubMed: 16000302]
42. DeJong J, Bernstein R, Roeder RG. Proc. Natl. Acad. Sci. U. S. A 1995;92:3313–3317. [PubMed: 7724559]
43. Xiao G, Cui Y, Ducy P, Karsenty G, Franceschi RT. Mol. Endocrinol 1997;11:1103–1113. [PubMed: 9212058]
44. Wang D, Christensen K, Chawla K, Xiao G, Krebsbach PH, Franceschi RT. J. Bone Miner. Res 1999;14:893–903. [PubMed: 10352097]
45. Jiang D, Franceschi RT, Boules H, Xiao G. J. Biol. Chem 2004;279:5329–5337. [PubMed: 14634012]
46. Wang J, Xi L, Hunt JL, Gooding W, Whiteside TL, Chen Z, Godfrey TE, Ferris RL. Cancer Res 2004;64:1861–1866. [PubMed: 14996750]
47. Willis DM, Loewy AP, Charlton-Kachigian N, Shao JS, Ornitz DM, Towler DA. J. Biol. Chem 2002;277:37280–37291. [PubMed: 12145306]
48. Xiao ZS, Liu SG, Hinson TK, Quarles LD. J. Cell. Biochem 2001;82:647–659. [PubMed: 11500942]
49. Xiao G, Jiang D, Thomas P, Benson MD, Guan K, Karsenty G, Franceschi RT. J. Biol. Chem 2000;275:4453–4459. [PubMed: 10660618]

50. Meyer T, Carlstedt-Duke J, Starr DB. J. Biol. Chem 1997;272:30709–30714. [PubMed: 9388207]
51. Lassot I, Estrabaud E, Emiliani S, Benkirane M, Benarous R, Margottin-Goguet F. J. Biol. Chem 2005;280:41537–41545. [PubMed: 16219772]
52. Garrett IR, Chen D, Gutierrez G, Zhao M, Escobedo A, Rossini G, Harris SE, Gallwitz W, Kim KB, Hu S, Crews CM, Mundy GR. J. Clin. Investig 2003;111:1771–1782. [PubMed: 12782679]
53. Zhao M, Qiao M, Harris SE, Oyajobi BO, Mundy GR, Chen D. J. Biol. Chem 2004;279:12854–12859. [PubMed: 14701828]
54. Frendo JL, Xiao G, Fuchs S, Franceschi RT, Karsenty G, Ducy P. J. Biol. Chem 1998;273:30509–30516. [PubMed: 9804819]
55. Dobreva G, Chahrour M, Dautzenberg M, Chirivella L, Kanzler B, Farinas I, Karsenty G, Grosschedl R. Cell 2006;125:971–986. [PubMed: 16751105]
56. Nakajima N, Horikoshi M, Roeder RG. Mol. Cell. Biol 1988;8:4028–4040. [PubMed: 3185540]
57. Buratowski S, Hahn S, Guarente L, Sharp PA. Cell 1989;56:549–561. [PubMed: 2917366]
58. Conaway RC, Conaway JW. Proc. Natl. Acad. Sci. U. S. A 1989;86:7356–7360. [PubMed: 2552440]
59. Maldonado E, Ha I, Cortes P, Weis L, Reinberg D. Mol. Cell. Biol 1990;10:6335–6347. [PubMed: 2247058]
60. Lavery DN, McEwan IJ. Biochem. Soc. Trans 2006;34:1054–1057. [PubMed: 17073749]
61. Kurihara N, Reddy SV, Araki N, Ishizuka S, Ozono K, Cornish J, Cundy T, Singer FR, Roodman GD. J. Bone Miner. Res 2004;19:1154–1164. [PubMed: 15176999]
62. Guo B, Aslam F, van Wijnen AJ, Roberts SG, Frenkel B, Green MR, DeLuca H, Lian JB, Stein GS, Stein JL. Proc. Natl. Acad. Sci. U. S. A 1997;94:121–126. [PubMed: 8990171]
63. Jurutka PW, Hsieh JC, Remus LS, Whitfield GK, Thompson PD, Haussler CA, Blanco JC, Ozato K, Haussler MR. J. Biol. Chem 1997;272:14592–14599. [PubMed: 9169418]
64. Newberry EP, Latifi T, Battaile JT, Towler DA. Biochemistry 1997;36:10451–10462. [PubMed: 9265625]
65. Hatta M, Yoshimura Y, Deyama Y, Fukamizu A, Suzuki K. Int. J. Mol. Med 2006;17:425–430. [PubMed: 16465388]
66. Clemens KE, Piras G, Radonovich MF, Choi KS, Duvall JF, DeJong J, Roeder R, Brady JN. Mol. Cell. Biol 1996;16:4656–4664. [PubMed: 8756622]

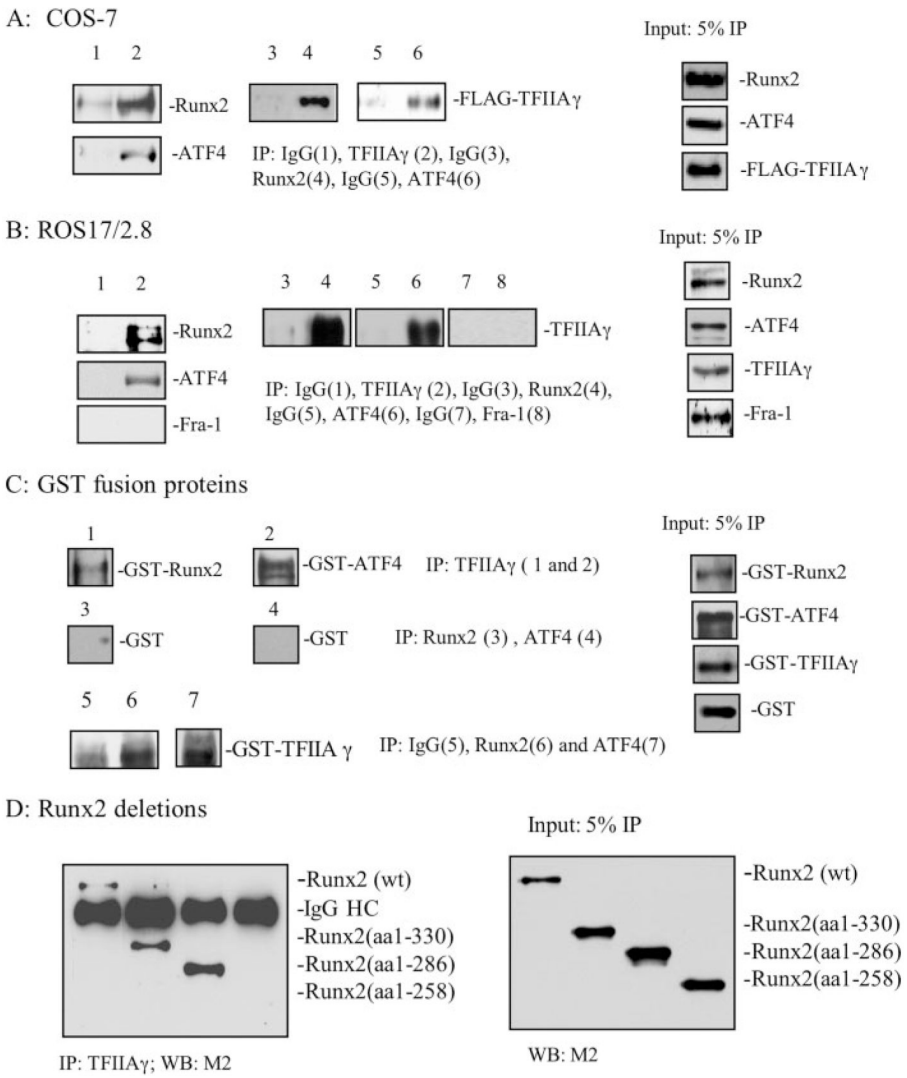

FIGURE 1. Protein-protein interactions among TFIIAγ, Runx2, and ATF4

A, whole cell extracts from COS-7 cells overexpressing pFLAG-TFIIAγ, pCMV-Runx2, and pCMV-ATF4 were immunoprecipitated (*IP*) with normal IgG (*lane 1*) or TFIIAγ antibody (*lane 2*) followed by Western blot (*WB*) analysis using Runx2 or ATF4 antibodies. In reciprocal IPs, the same extracts were immunoprecipitated with normal IgG (*lanes 3* and *5*), Runx2 antibody (*lane 4*), or ATF4 antibody (*lane 6*) followed by WB using M2 antibody. *B*, nuclear extracts from ROS17/2.8 cells were immunoprecipitated with normal IgG (*lane 1*) or TFIIAγ antibody (*lane 2*) followed by WB using Runx2, ATF4, or Fra-1 antibodies. In reciprocal IPs, the same extracts were immunoprecipitated with normal IgG (*lanes 3*, *5* and *7*), Runx2 antibody (*lane 4*), ATF4 antibody (*lane 6*), or Fra-1 antibody (*lane 8*) followed by WB using TFIIAγ antibody. *C*, mixture of purified GST-TFIIAγ and GST-Runx2 was immunoprecipitated by TFIIAγ antibody followed by WB for Runx2 (*lane 1*). A mixture of purified GST-TFIIAγ and GST-ATF4 was immunoprecipitated by TFIIAγ antibody followed by WB for ATF4 (*lane 2*). A mixture of purified GST and GST-Runx2 was immunoprecipitated by Runx2 antibody followed by WB for GST (*lane 3*). A mixture of purified GST and GST-ATF4 was immunoprecipitated by ATF4 antibody followed by WB for GST (*lane 4*). In reciprocal IPs, a mixture of purified GST-TFIIAγ and GST-Runx2 was immunoprecipitated by normal IgG (*lane 5*) or Runx2 antibody (*lane 6*) followed by WB for TFIIAγ. A mixture of

purified GST-TFIIAγ and GST-ATF4 was immunoprecipitated by ATF4 antibody (*lane 7*) followed by WB for TFIIAγ. *D*, nuclear extracts from ROS17/2.8 cells were mixed with equal amount of nuclear extracts from COS-7 cells overexpressing FLAG-Runx2(wt), FLAG-Runx2 (aa 1–330), FLAG-Runx2 (aa 1–286), and FLAG-Runx2 (aa 1–258), and immunoprecipitated with TFIIAγ antibody followed by WB for Runx2 (M2 antibody). Experiments were repeated 2–3 times, and qualitatively identical results were obtained

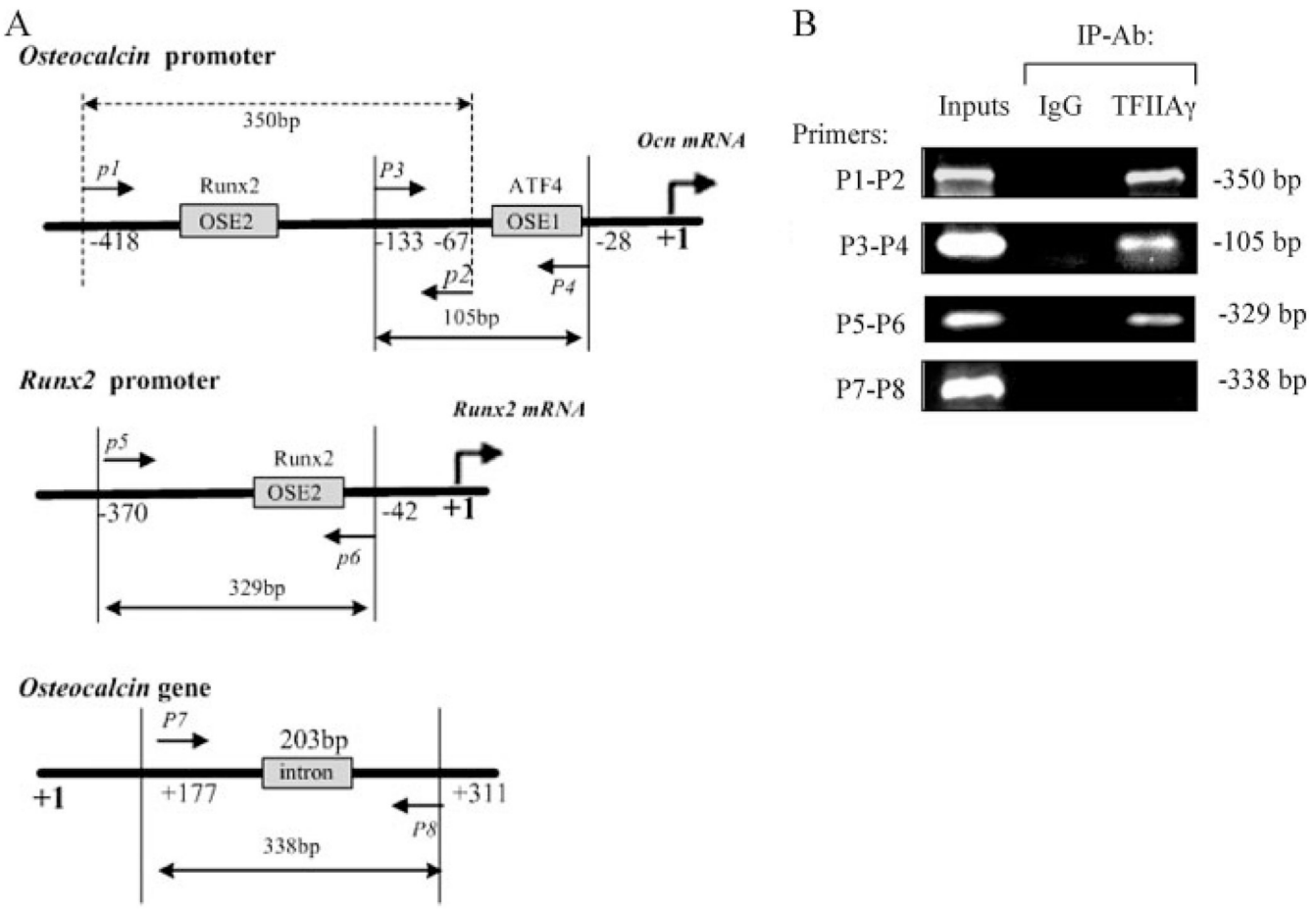

FIGURE 2. ChIP analysis of TFIIAγ interaction with Runx2/ATF4 binding sites-containing chromatin fragments of *mOG2* promoter in MC-4 cells

A, schematic representation of relevant regions of the *mOG2* promoter, mouse *Runx2* promoter, and *mOG2* gene. P1, P2, P3, P4, P5, P6, P7, and P8 indicate PCR primers used to analyze ChIP DNAs. The positions of these primers and the size of the fragments they amplify are indicated at the top or bottom of the figure. *B*, MC-4 cells were seeded at a density of 50,000 cells/cm^2 in 35-mm dishes, cultured in 10% FBS medium overnight, and cross-linked with formaldehyde for ChIP assays. IPs were conducted with TFIIAγ antibody (*Ab*) or normal control IgG. PCR products were run on 3% agarose gel and stained with ethidium bromide. Purified input chromatin was used to perform parallel PCRs with the respective primer pairs. Experiments were repeated three times with similar results.

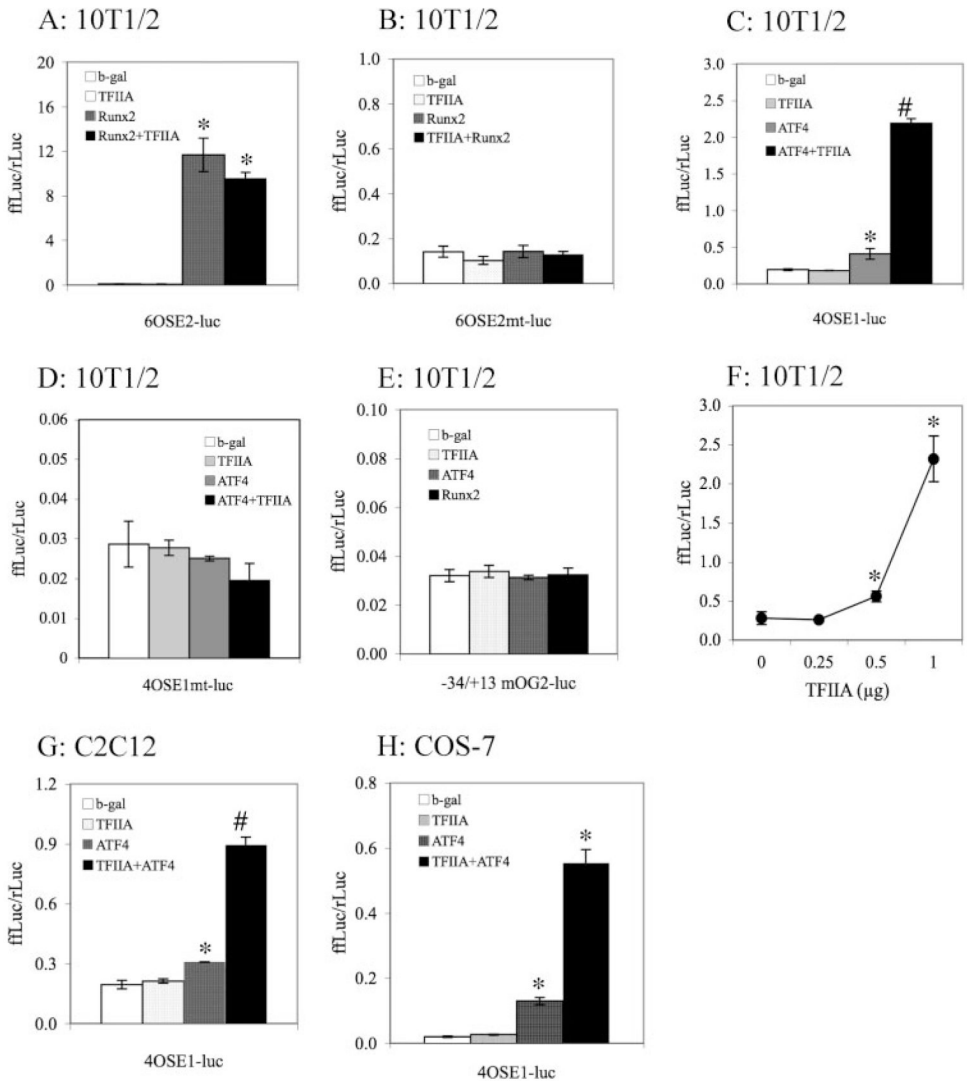

FIGURE 3. TFIIAγ increases ATF4 but not Runx2 transcriptional activity

A and *B*, 10T1/2 cells were transiently transfected with p6OSE2-luc (*A*) or p6OSE2mt-luc (*B*) and pRL-SV40 (for normalization) and expression plasmids for β-galactosidase, TFIIAγ, Runx2, or Runx2 plus TFIIAγ. After 36 h, cells were harvested for dual luciferase assay. Firefly luciferase was normalized to *Rotylenchulus reniformis* luciferase to control the transfection efficiency (*, $p < 0.01$(β-galactosidase *versus* Runx2 or Runx2 + TFIIAγ). *C* and *D*, 10T1/2 cells were transiently transfected with p4OSE2-luc (*C*) or p4OSE1mt-luc (*D*) and pRL-SV40 and expression plasmids for β-galactosidase, TFIIAγ, ATF4, or ATF4 plus TFIIAγ. *, $p < 0.01$ (β-galactosidase *versus* ATF4 or ATF4 + TFIIAγ); #, $p < 0.01$(ATF4 *versus* ATF4 + TFIIAγ). *E*, 10T1/2 cells were transiently transfected with −34/+13 mOG2-luc and pRL-SV40 and expression plasmids for β-galactosidase, TFIIAγ, ATF4, or Runx2. *F*, dose-response experiment, 10T1/2 cells were transiently transfected with p4OSE1-luc and pRL-SV40 and ATF4 expression plasmid and increasing amounts of TFIIAγ plasmid. *, $p < 0.01$ (β-galactosidase *versus* TFIIAγ).*G* and *H*, C2C12 (*G*) and COS-7 cells (*H*) were transiently transfected with p4OSE2-luc and pRL-SV40 and expression plasmids for β-galactosidase, TFIIAγ, ATF4, or ATF4 plus TFIIAγ. *, $p < 0.01$ (β-galactosidase *versus* ATF4 or ATF4 + TFIIAγ). Data represent mean ± S.D. Experiments were repeated three times and qualitatively identical results were obtained. Note the expanded scale for the mutant reporters (*B*, *D*, and

E) because of low basal activity to enable visualization of any potential differences as a consequence of cotransfection with the expression vectors noted above.

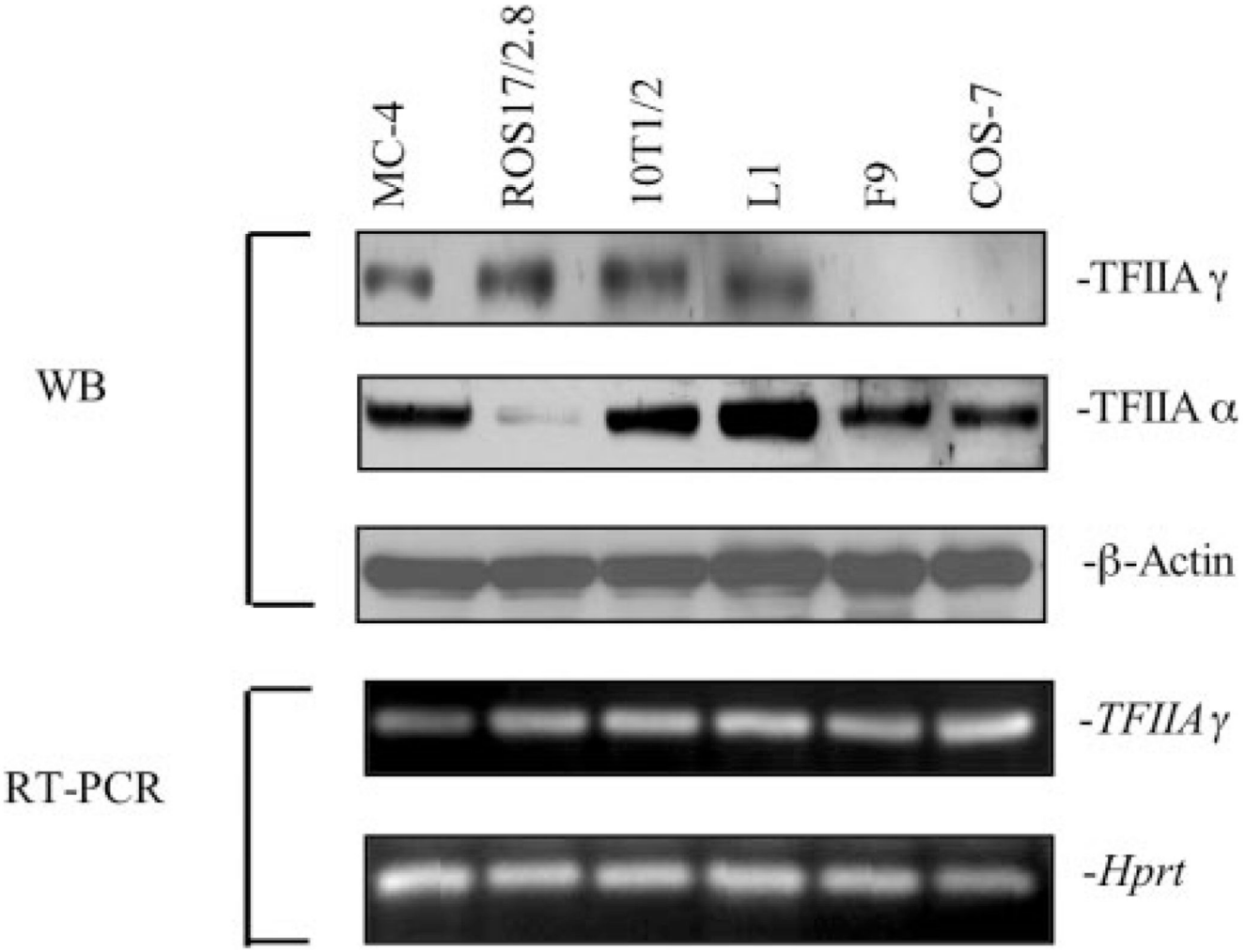

FIGURE 4. TFIIAγ expression in different cell lines

Total RNAs or whole cell extracts were prepared from MC-4, ROS17/2.8, 10T1/2, L1, F9, and COS-7 cells and used for RT-PCR and Western blot analysis for levels of TFIIAα and TFIIAγ mRNAs and proteins. Experiments were repeated three times with similar results.

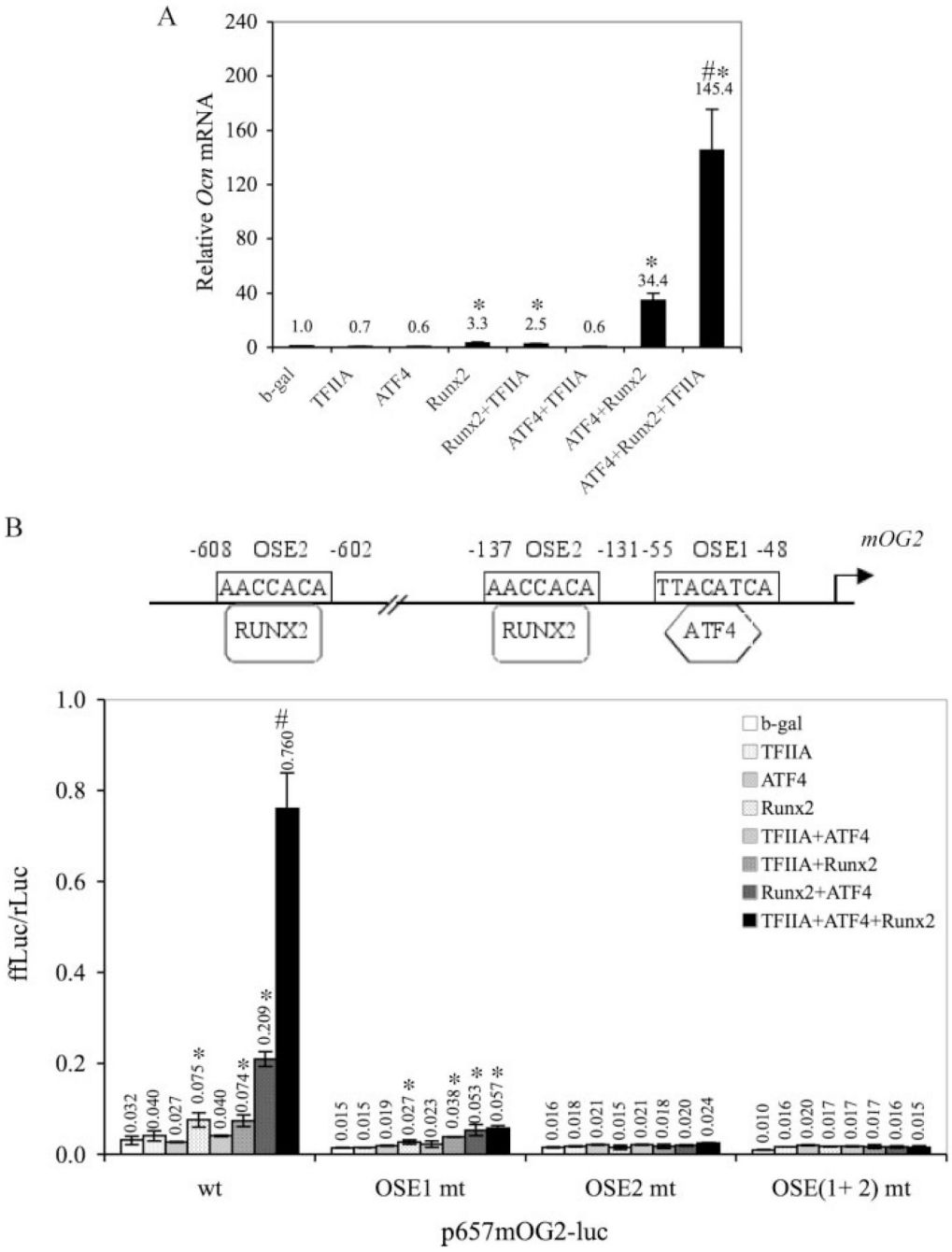

FIGURE 5. TFIIAγ activates endogenous *Ocn* gene expression and 0.657-kb *mOG2* promoter activity in the presence of ATF4 and Runx2

A, 10T1/2 cells were transfected with expression plasmids forβ-galactosidase (β-*gal*), TFIIAγ, ATF4, Runx2, Runx2/TFIIAγ, ATF4/TFIIAγ, ATF4/Runx2, or ATF4/TFIIAγ/Runx2. After 36 h, the cells were harvested for RNA isolation and quantitative real time RT/PCR analysis for *Ocn* mRNA. *B*, 10T1/2 cells were transfected with p657mOG2-luc or p657mOG2OSE1mt-luc or p657mOG2OSE2mt-luc or p657mOG2OSE(1 + 2)mt-luc, pRL-SV40, and expression plasmids for β-galactosidase, TFIIAγ, ATF4, Runx2, Runx2/TFIIAγ, ATF4/TFIIAγ, ATF4/Runx2, or ATF4/TFIIAγ/Runx2. After 36 h, the cells were harvested for dual luciferase assay. *, $p < 0.01$ (β-galactosidase *versus* Runx2, or ATF4 + Runx2 or ATF4

+ Runx2 + TFIIAγ); #, $p < 0.01$(ATF4 + Runx2 *versus* ATF4 + Runx2 + TFIIAγ). Data represent mean ± S.D. Experiments were repeated 3–4 times and qualitatively identical results were obtained.

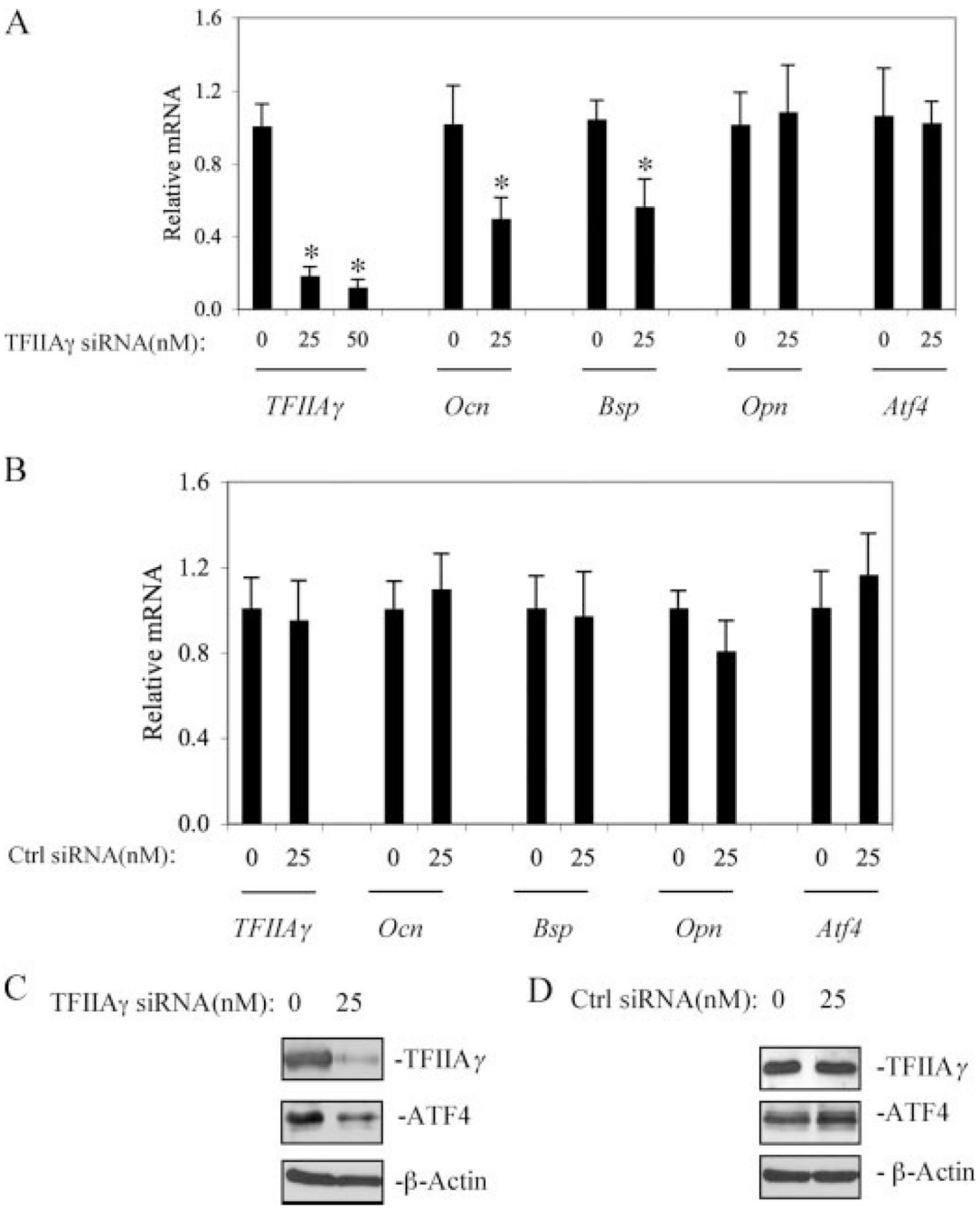

FIGURE 6. TFIIAγ siRNA blocks endogenous *Ocn* mRNA expression in osteoblastic cells

ROS17/2.8 osteoblast-like cells were transiently transfected with *TFIIA*γ siRNA (*A*) or negative control (*Ctrl*) siRNAs (*B*). After 36 h, total RNA or whole cell extracts were prepared for quantitative real time RT-PCR analysis for *TFIIA*γ, *Ocn*, *Bsp*, *Opn*, and *Atf4* mRNAs which were normalized to the 18 *S rRNA* mRNAs or Western blot analysis for ATF4, TFIIAγ, and β-actin (*C* and *D*). *, $p < 0.01$ (control *versus* siRNA). Data represent mean ± S.D. Experiments were repeated three times with similar results.

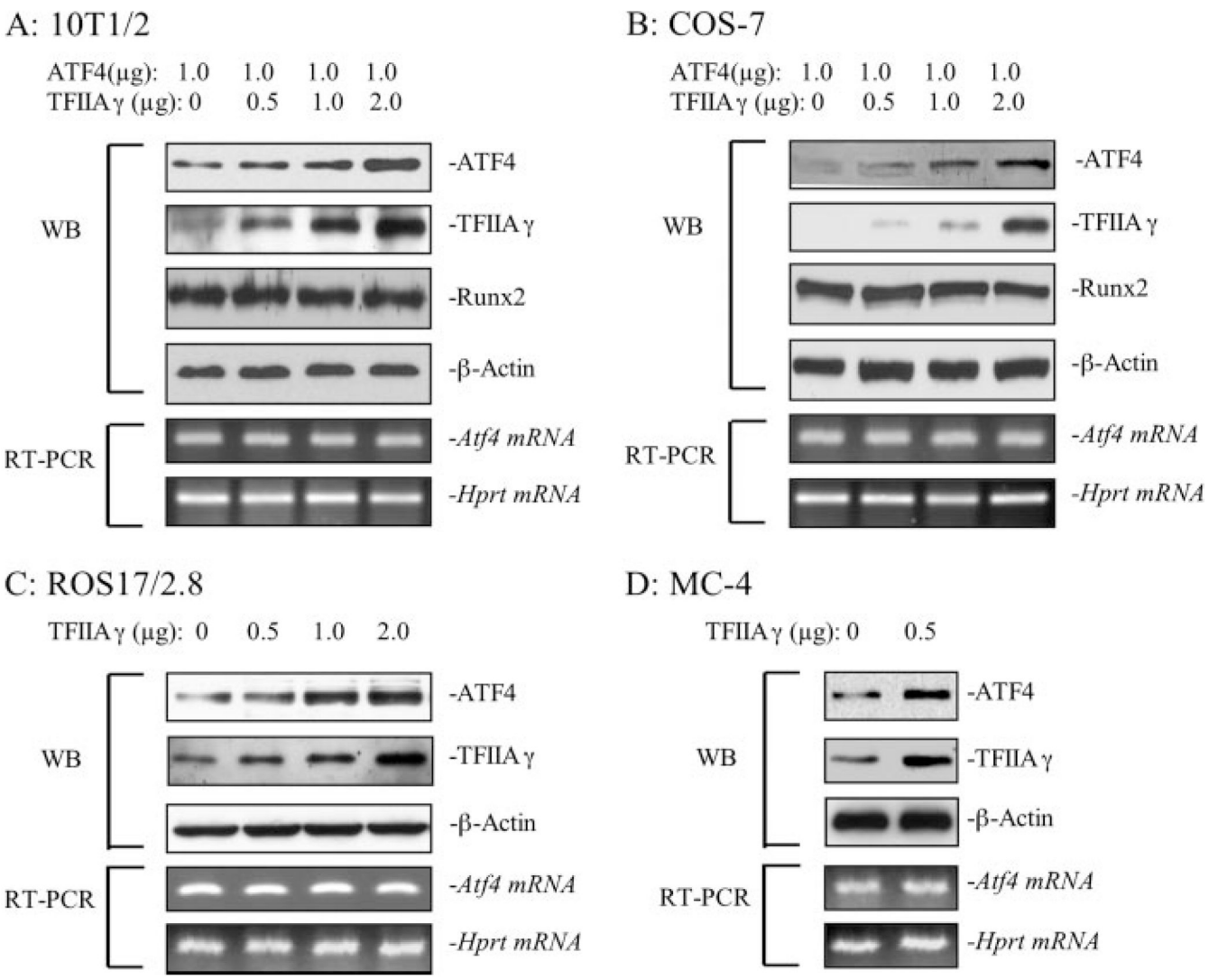

FIGURE 7. TFIIAγ increases the levels of ATF4 protein

C3H10T1/2 (*A*) and COS-7 (*B*) cells were transfected with 1 μg of pCMV/ATF4 or pCMV/Runx2 and increasing amounts of FLAG-TFIIAγ expression vector (0, 0.5 1, 2 μg) followed by Western blotting for ATF4, TFIIAγ, Runx2, and β-actin (*top*) or RNA preparation and RT-PCR for *Atf4* and *Hprt* mRNA (*bottom*). ROS17/2.8 (*C*) and MC-4 (*D*) cells were transfected with increasing amounts of FLAG-TFIIAγ expression vector (0, 0.5, 1, and 2 μg). Experiments were repeated three times with similar results.

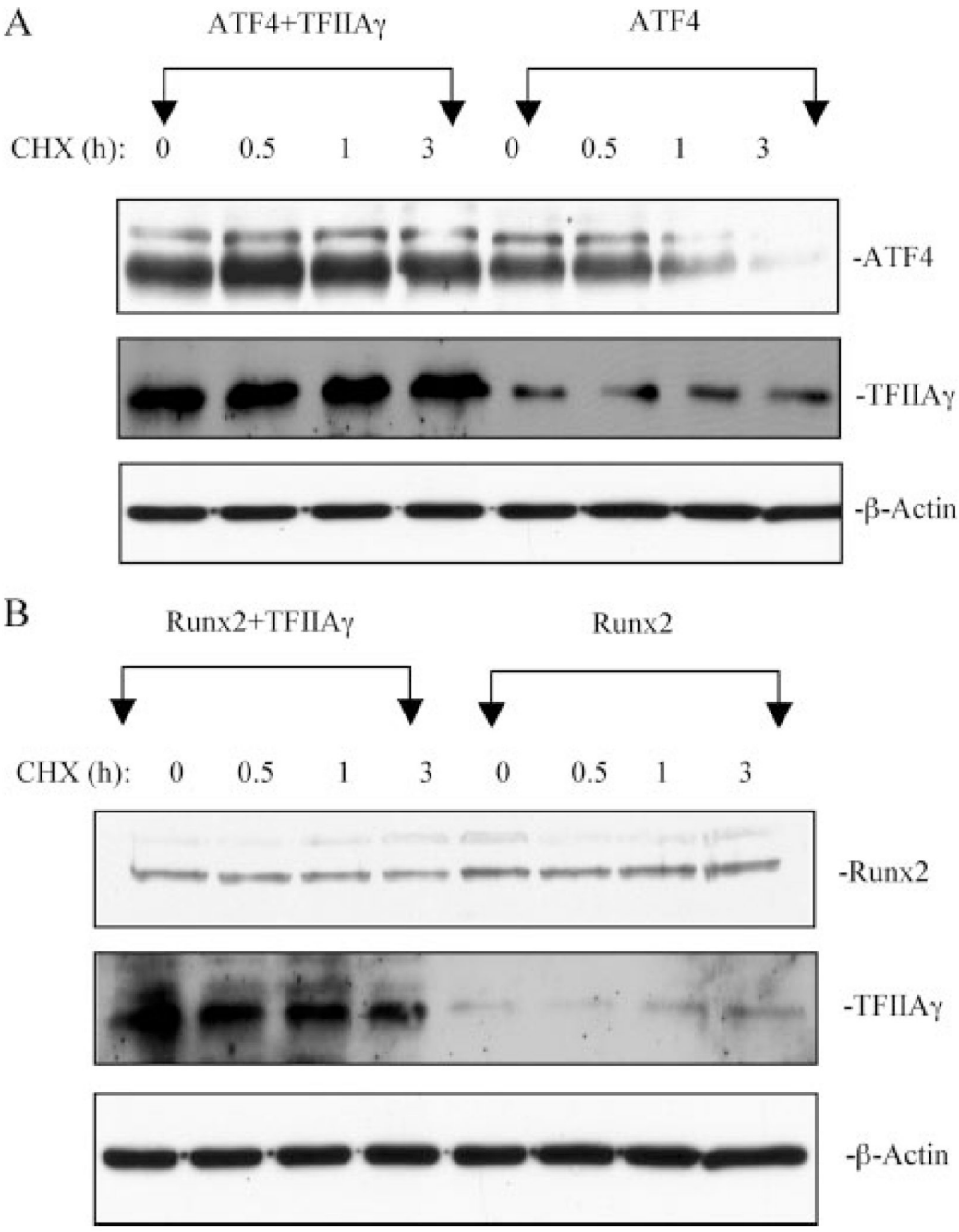

FIGURE 8. TFIIAγ increases ATF4 protein stability

C3H10T1/2 cells were transfected with 1.0 μg ATF4 (*A*) or Runx2 (*B*) expression vector with and without 1.0 μg of TFIIA expression vector. After 36 h, cells were treated with 50 μg/ml of protein synthesis inhibitor cycloheximide (*CHX*) and harvested at different time points (0, 1, and 3 h) followed by Western blot analysis for ATF4 and Runx2. Experiments were repeated three times with similar results.

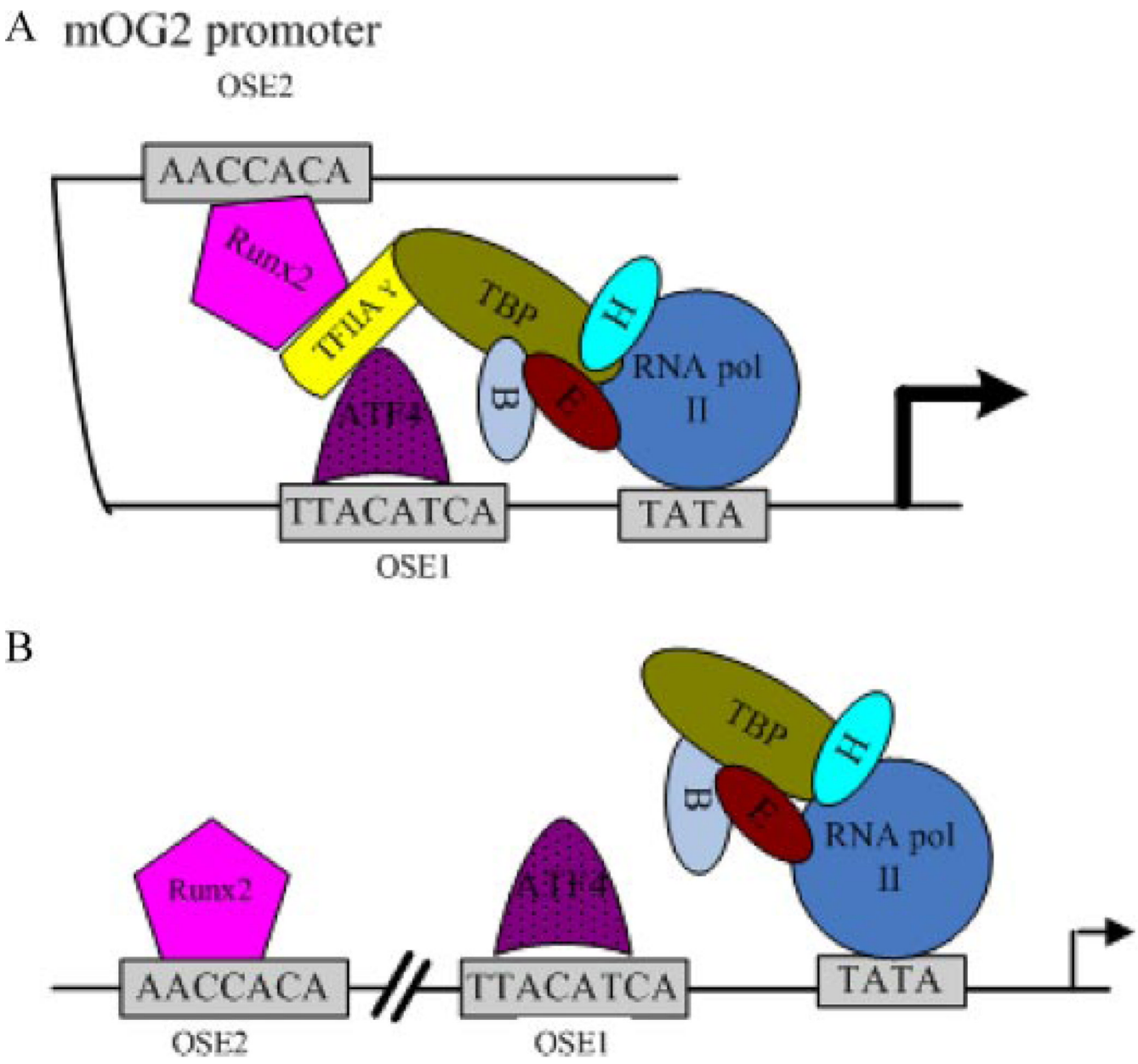

FIGURE 9. Role of TFIIAγ in osteoblast-specific *Ocn* gene expression

In osteoblasts, when the level of TFIIAγ is high (*A*), ATF4 and Runx2 are recruited to the transcriptional initiation complex of the *mOG2* promoter through direct binding to TFIIAγ, which in complex with RNA polymerase II and many other basal transcription factors and/or cofactors, including TFIIA, TFIIB, TBP (TFIID), TFIIE, TFIIF, and TFIIH, leads to an increase in transcription. In contrast, when the level of TFIIAγ is low (*B*), ATF4 and Runx2 are not recruited to the basal transcriptional machinery, resulting in a decrease in transcription. Level of TFIIAγ can be regulated by factors to be defined.

TABLE 1

PCR primers used in ChIP assay

Oligonucleotide name	Sequence
P1	CCGCTCTCAGGGGCAGAC
P2	AGGGGATGCTGCCAGGACTAAT
P3	CACAGCATCCTTTGGGTTTGAC
P4	TATCGGCTACTCTGTGCTCTCTGA
P5	GCTATA ACCTTCTT AATGCCAG
P6	AGCACTATTACTGGAGAGACAGAATC
P7	TAGTGAACAGACTCCGGCGCTA
P8	TGTAGGCGGTCTTCA AGCCAT